



## **Current State of Defect Review by Electron Beam Tools: A White Paper**

**SEMATECH** and the **SEMATECH logo** are registered service marks of SEMATECH, Inc.  
**International SEMATECH** and the **International SEMATECH logo** are registered service marks  
of International SEMATECH, Inc., a wholly-owned subsidiary of SEMATECH, Inc.

Product names and company names used in this publication are for identification purposes only  
and may be trademarks or service marks of their respective companies.

# Current State of Defect Review by Electron Beam Tools:

## A White Paper

Technology Transfer # 00013877A-ENG

SEMATECH

January 14, 2000

**Abstract:** This white paper examines the performance of electron beam (E-beam) tools for defect review at the 0.14  $\mu\text{m}$  node and beyond, using a statistical model of contrast formation to estimate error rates and detection limits, on the basis of the electron-optical performance of the tool. It is found that while there is no problem in detecting defects as small as 10 nm even when using current instrumentation, the throughput rate is too slow to meet the required specification for imminent technology generations. Possible strategies to circumvent this limitation are discussed.

**Keywords:** Defect Detection, Electron Beam Columns, Equipment Performance, Statistical Modeling

**Authors:** Alain Diebold, David Joy

**Approvals:** Alain Diebold, Author  
Robin Worley, Project Manager  
Ron Remke, Program Manager  
Rinn Cleavelin, Director, Front End Processes  
Dan McGowan, Technical Information Transfer Team Leader



## Table of Contents

1	EXECUTIVE SUMMARY .....	1
2	INTRODUCTION.....	1
3	CURRENT RESEARCH .....	2
3.1	Major Suppliers of E-Beam Defect Review and Defect Imaging Tools.....	3
3.2	Key Figures in the Field of Instrumentation Development .....	3
3.3	Limitations of Electron Beam Imaging .....	3
3.4	Model for Defect Detection .....	3
4	APPLICATION OF THEORY TO DEFECT REVIEW TOOLS.....	7
4.1	What Can be Done to Improve the Performance.....	8
4.1.1	Brighter Electron Sources .....	9
4.1.2	Electron–Optical Improvements .....	9
4.1.3	Better Detectors.....	10
4.1.4	Multiple Columns/Detectors .....	10
5	CONCLUSIONS.....	11
5.1	Is There An Alternative?.....	11
6	REFERENCES.....	12

## List of Figures

Figure 1	Variation of the Error Rate for Defect Detection with the Imaging Parameter $p = \{(S/N).Contrast\}$ .....	4
Figure 2	Variation of the Signal-to-Noise (S/N) Ratio for a Silicon Specimen Observed at 2 keV as a Function of the Incident Beam Current and the Pixel Dwell Time .....	5
Figure 3	Theoretical <i>OTF</i> for the Case of a Beam Probe with a Gaussian Width Equal to 1 Pixel in Size .....	6
Figure 4	Computed Error Rates as a Function of Defect Size (in Pixels).....	7



## 1 EXECUTIVE SUMMARY

This white paper examines the performance of electron beam (E-beam) tools for defect review at the 0.14  $\mu\text{m}$  node and beyond, using a statistical model of contrast formation to estimate error rates and detection limits, on the basis of the electron-optical performance of the tool. It is found that while there is no problem in detecting defects as small as 10 nm even when using current instrumentation, the throughput rate is three to four orders of magnitude too slow to meet the required specification for imminent technology generations. Possible strategies to circumvent this limitation are discussed, with the following results:

1. The SEMATECH specification set for the detection of small (<100 nm) at acceptable error rates can be met readily using technology that is already available.
2. However, the scanning rate that is possible for such sub-100 nm defects is about three to four orders of magnitude slower than required.

An analysis of the options available shows that this gap can be partially closed as follows:

1. By using higher brightness electron sources such as nanotip field emitters, offering a factor of up to 10X in speed
2. By employing advanced lenses and electron-optical schemes, such as retarding field cathode lenses, possibly yielding another factor of 10X in scan speeds

Finally, this paper finds that an alternative approach may exist in the use of reflection electron holography performed in a point protection microscope. While significant issues exist in this areas, point projection holography might provide a defect review technique that could deal with any technology node yet envisaged.

## 2 INTRODUCTION

State-of-the-art optical detection equipment presently is not capable of capturing sub-100 nm defects on patterned wafers, and there is also a steep dropoff in the throughput of such tools when their sensitivity is enhanced to detect smaller defect sizes. Thus, although optical techniques have been the mainstay of semiconductor defect detection, it is not clear that they will continue to be as useful in the newer technology generations (for a good general review of current defect review techniques see Brundle et al., 1998 [1]). Increasing attention therefore is being given to electron beam techniques, based on the architecture of the scanning electron microscope (SEM), which by contrast can offer high sensitivity, but which offers limited throughput because of the sequential nature of its operation, and because of fundamental signal-to-noise constraints.

Defect detection applications typically do not demand the ability to resolve features. Rather, the emphasis is on scan speed so that a large area can be “looked at” within a specified time period and a list of all locations in the area that are suspected of being defective then can be reported for further examination. Often, this is achieved by exploiting the voltage contrast mechanism of image formation under conditions of low voltage E-beam irradiation. The charge distribution is imaged and compared to the adjacent dies/cells or to a “golden” die/cell. The highest speed of reliably detecting defects by this method is reported to be only 6  $\text{cm}^2$  per hour at a sensitivity level of 150 nm. Although this is slower than ideally required, the high correlation of detected defects to “killers” outweighs the negative aspect of the lack of absolute speed for this technology. Recognizing, however, that such a speed is most certainly not sufficient for high

volume defect detection in future device generations, this white paper aims to survey current limitations in the technology and hence to identify new techniques that can overcome these constraints. By doing so, this paper aims to identify a complementary methodology to optical platforms, enabling a more exhaustive determination of possible faults early in the process flow and improving yield learning and profitability.

In order to provide enhanced IC performance characteristics, new materials and processing will be introduced over the next several technology nodes. Transistor structures will need to incorporate alternate gate dielectric (and possibly gate electrode) materials, and these new materials may force new process flows such as “replacement gates” that avoid thermally altering the new dielectric material. Interconnect structures will be made by etching trench and contact openings in the insulator and filling them with barrier layer and copper metals. The aspect ratio continues to grow with each technology generation. The insulator dielectric constant is lower for each subsequent IC generation, thus a new material must be employed. In addition, the low  $k$  insulator eventually will become porous when available materials do not meet dielectric constant requirements. Thus, a successful strategy for future defect detection technology must include tactics that test potential methods for their non-destructiveness, using the appropriate materials set.

### **3 CURRENT RESEARCH**

Significant recent research has been made into several key areas of E-beam defect review with the aim of increasing sensitivity and throughput. One major advance has been the nearly universal replacement of thermionic electron emitters with field emission guns. Although some suppliers (KLA, OPAL, Schlumberger) have favored the Schottky emitter because of its high output and good long-term stability, cold field emitters also have been employed because of their superior performance at low beam energies (Hitachi). The use of field emitters results in a significantly higher current density in the probe and consequently more current into a probe of given size, and the higher current also permits faster scan speeds. There also have been advances in the probe lens design, for example the adoption of so-called Snorkel (or field projection) lenses that combine good aberrations with excellent specimen access. The desire for better aberration performance is driven not so much by the need for a small probe size, as by the requirement of getting as much current as possible into a probe of given diameter to reduce error rates and enhance scanning speeds.

The performance of the lens can be enhanced still further by applying a negative potential to the wafer so that, in combination with the objective, a cathode-lens is formed (Hordon et al., 1995 [2]). This decelerates the incoming electron beam, allowing the landing energy to be set easily to any desired figure, and reduces the effective lens aberrations by a factor of as much as ten times. Advantage also has been taken of the magnetic field emerging from the objective lens by employing it to capture the secondary electrons from the sample. After being allowed to pass through the lens the secondary electron (SE) signal can then be separated from the incident beam by a Wien filter in the optical path. Compared to the conventional Everhart-Thornley SE detector system, this arrangement offers highly efficient SE detection, uniform illumination across the field of view, high sensitivity to voltage contrast effects, and good discrimination between different types of emitted electron signals.

In addition to dedicated E-beam defect review tools, some suppliers (JEOL, Hitachi) have introduced defect imaging microscopes that can offer high resolution imaging of tilted samples for the study and microanalysis of defects, in addition to automatic defect detection and classification. Such tools can be regarded as a hybrid between laboratory-grade SEM and specialized defect review tools.

### 3.1 Major Suppliers of E-Beam Defect Review and Defect Imaging Tools

Suppliers and their websites are as follows:

KLA-Tencor	<a href="http://www.kla-tencor.com">http://www.kla-tencor.com</a>
OPAL (Applied Materials)	<a href="http://www.appliedmaterials.com">http://www.appliedmaterials.com</a>
Hitachi	<a href="http://www.nissei.com">http://www.nissei.com</a>
JEOL	<a href="http://www.jeol.com">http://www.jeol.com</a>
Schlumberger ATE	<a href="http://www.slb.com/ate/">http://www.slb.com/ate/</a>
FEI/Philips/Micrion	<a href="http://www.feic.com">http://www.feic.com</a>

### 3.2 Key Figures in the Field of Instrumentation Development

Major contributions to the field have been made by Lee Venerklassen (now of ETEC) in the design of high performance field emitters; by Eric Munro (of Munro Electron Beam Software Ltd.) in the computer design and simulation of electron-optical systems; by Philip Chang (now of ETEC) in the design of microcolumns and arrays of columns; and by members of Professor Fabian Pease's group at Stanford in the design and characterization of advanced optical systems.

### 3.3 Limitations of Electron Beam Imaging

Elementary electron optics determine the level of performance available for a given beam voltage and specified spatial resolution. In particular, because the brightness of electron sources increases linearly with beam energy and because the aberrations of lenses get worse at lower energies, the currents available at a low beam energy (such as 1 keV into a 10–20 nm spot) are substantially smaller than those attainable at 20 or 30 keV. This appears to imply that defect detection might more efficient at higher voltages, even though the trend of the industry has been to use incident energies that are as low as possible so as to minimize charging, or irradiation damage, to gate oxides. This topic will be discussed later.

### 3.4 Model for Detect Detection

Under certain conditions, a defect does not need to be imaged to be detected, e.g., the case of detection on repeated patterns. The only requirement is that the signal change corresponding to the presence of the defect be significant enough to be reliably discriminated from the noise. The ability of a SEM to detect a defect of a given size then is determined by the diameter of the electron probe and by the signal-to-noise ratio of the image. If either of these factors is unsatisfactory, then detection will be unreliable or impossible. This section will develop a simple model to demonstrate how the error rate of defect detection varies with the operational parameters of the tool. It will be assumed that the error rate and the speed of defect detection is set only by the requirement that the tool deliver sufficient electrons to the sample, and not by factors such as the performance of subsequent image analysis software and hardware.

Consider a defect that generates a signal change of value  $\Delta S$  around the average signal level of  $S$ , when the beam scans across it. The probability that this signal change  $\Delta S$  could have occurred as a result of random noise depends on the ratio of  $\Delta S$  to the noise  $N$ . The error rate of the detection process is therefore a function  $f(\cdot)$  of the ratio described in Equation [1].

For the purposes of analysis, it is easier to rewrite Eq. [1] in the form:

$$Error = f\left(\frac{\Delta S}{N}\right) \quad \text{Eq. [1]}$$

$\Delta S/S$  is then the contrast or visibility of the defect, while  $S/N$  is the signal-to-noise ratio.

$$Error = f\left(\frac{\Delta S}{N} \cdot \frac{S}{N}\right) \quad \text{Eq. [2]}$$

On the assumption that this error has a normal (i.e., Gaussian) distribution, Figure 1 plots the error rate for detection as a function of the parameter  $\mathbf{p} = \{(\Delta S/S) \cdot (S/N)\}$ . The error rate is seen to vary over several orders of magnitude for a modest change in the value of the quantity  $\mathbf{p}$ . For example, when this parameter is 4 or higher, the error rate is below 0.01%, but when the parameter  $\mathbf{p}$  is reduced to unity the error rate (i.e., the chance that the observed signal level could be the result of a random fluctuation) rises to nearly 20%, while for still lower values of  $\mathbf{p}$  the error rate becomes 50%, at which level the detection probability is no better than purely random chance.

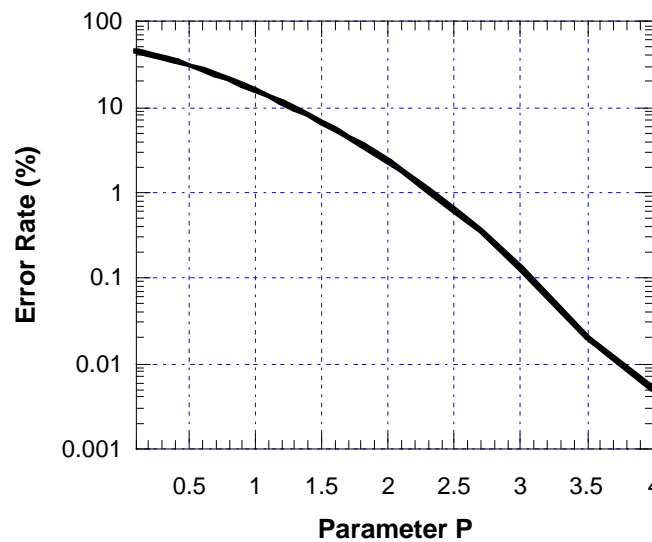


**Figure 1** Variation of the Error Rate for Defect Detection with the Imaging Parameter  $\mathbf{p} = \{(S/N) \cdot \text{Contrast}\}$

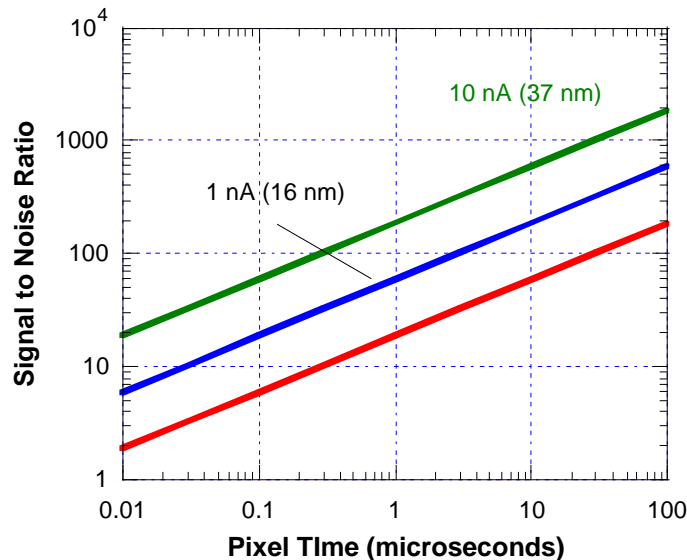
The performance of the defect review tool therefore will depend critically on the value of the parameter  $\mathbf{p}$  and hence on the values of 1) the contrast ( $\Delta S/S$ ) of the defect and 2) on the  $S/N$  ratio of the tool. For the purposes of this simplified discussion, it will be assumed that the contrast of the defect is constant at about 0.1 (i.e., 10%; see for example KLA 1996), although in practice it can be anticipated that the contrast would vary with defect type and size.

The S/N ratio depends on two terms. If the incident beam current is  $I_B$  (value in pico-amps), and if the time per pixel is  $\tau$  (value in microseconds), then the static S/N ratio  $S/N(0)$  is:

$$\frac{S}{N}(0) = \sqrt{6 \cdot DQE \cdot \tau \cdot \delta \cdot \frac{I_B}{e}} \quad \text{Eq. [3]}$$

where  $e$  is the charge on an electron ( $1.6 \cdot 10^{-19} \text{C}$ ),  $\delta$  is the secondary electron yield, and *detector quantum efficiency (DQE)* is the quantum efficiency of the detector being used to collect the signal. For a perfect detector  $DQE = 1$ , but typical secondary electron detectors on current SEM-based have *DQEs* measured in the range 0.2–0.9 (Joy et al., 1996 [4]).

Figure 2 plots the variation in S/N as function of the pixel dwell time for incident beam currents of 0.1, 1, and 10 nA, assuming that the specimen under examination is essentially silicon, that the *DQE* is 0.5, and that the beam energy is 2 keV. The S/N ratios for typical pixel times of the order of 0.1 to 1  $\mu\text{s}$  are seen to vary from about 10 to 200, depending on the incident beam current level. Note that, for the observation of silicon based materials, maintaining the same beam current value but dropping the beam voltage to 1 keV would improve the S/N ratio by about 30% compared to the 2 keV value, while raising the beam energy to 20 keV would reduce the S/N by almost 100% compared to 2 keV, because of the energy variation of the SE yield  $\delta$  (for tabulated values see Joy 1999 [3]).



Note: The annotations on the current values show the corresponding beam spot size assuming a source with a brightness of  $10^6$  amps/cm<sup>2</sup>/str. and a lens with a  $C_s$  of 5 mm.

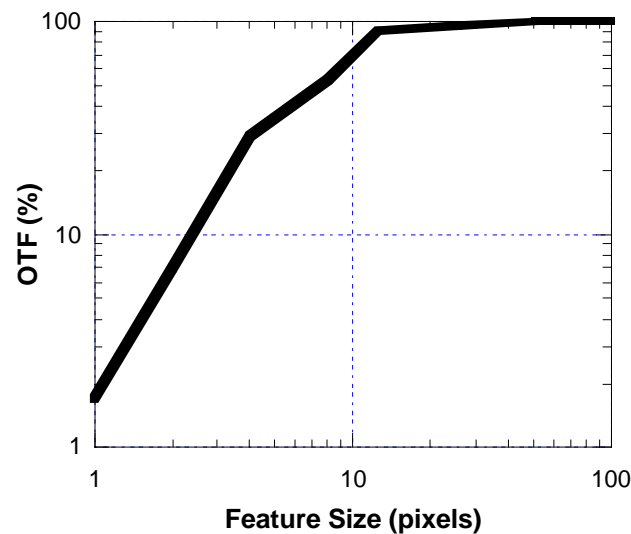
**Figure 2** Variation of the Signal-to-Noise (S/N) Ratio for a Silicon Specimen Observed at 2 keV as a Function of the Incident Beam Current and the Pixel Dwell Time

The effective S/N ratio of the system for detail in the image at some spatial frequency  $\omega$  then is given as:

$$\frac{S}{N}(\omega) = \frac{S}{N}(0) \cdot OTF(\omega) \quad \text{Eq. [4]}$$

where  $OTF(\omega)$  is the optical transfer function of the tool at the modulation frequency  $\omega$ . The  $OTF$  represents the relative response of the tool to the different spatial frequencies passing through it, and ideally  $OTF(\omega)$  would be equal to unity for all frequencies from DC upwards. In practice, the  $OTF$  is unity at low frequencies but falls rapidly at higher spatial frequencies (i.e., for the highest resolution detail in an image), ultimately reaching zero at the information cutoff limit of the tool. The form of the  $OTF$  vs. frequency plot in the simplest case would be the modulus of the Fourier transform of the electron beam profile at the sample surface, but on real microscopes other factors are also important, and these will still further depress the  $OTF$  value at higher spatial frequencies.

To illustrate the effect of these considerations, consider the example of a tool that is performing a defect review by scanning an image field of  $512 \times 512$  pixels. Assume that the beam spot diameter of the tool is 1 pixel in size. In the simplest case (i.e., assuming that the bandwidth and slew rate of the detectors and video amplifiers in the tool to be infinitely high), the  $OTF$  of this tool then would have the form shown in Figure 3.

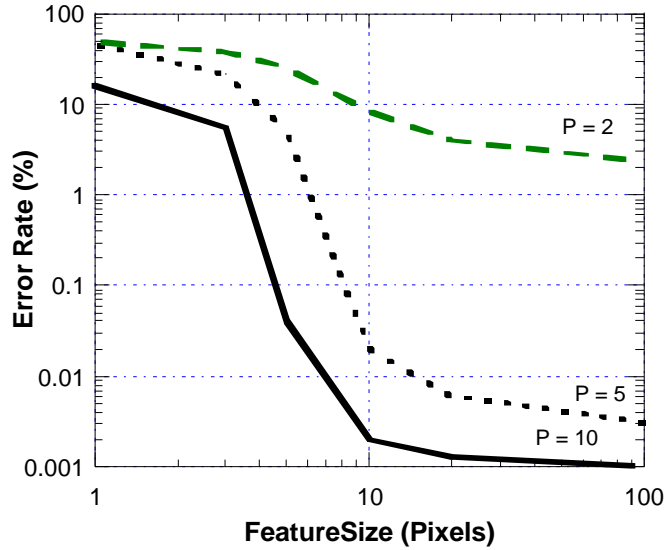


Note: The profile assumes that the bandwidth and slew rates of the amplifiers are not otherwise limiting the performance of the tool.

**Figure 3** Theoretical  $OTF$  for the Case of a Beam Probe with a Gaussian Width Equal to 1 Pixel in Size

Under these assumptions, it can be seen that the  $OTF$  for a feature 10 pixels in size is 0.7 (i.e., 70 % of maximum), but the  $OTF$  falls to only 0.15 for a 3 pixel object, 0.07 for a 2 pixel feature, and 0.02 for a 1 pixel-sized object. As a consequence of Eq. [4], the signal-to-noise ratio of the image therefore declines rapidly at the highest spatial frequencies, ultimately reaching a level where the error rate is too high to be of use.

Figure 4 shows the error rate for the detection of defects as a function of the defect size using Eq. [4] and the data of Figure 1 and for some typical values of the parameter  $p$ . For a specific example, let it be specified that the contrast of a defect has a constant value of 0.1 (i.e., 10 %). If the static S/N ratio of the system is 20, then the parameter  $p$  in Eq. [2] has a value of 2. Thus from Figure 4, defect 10 pixels in size could be detected with an error rate of just 10%, but the error would rise to nearly 50% for defects 3 pixels or smaller in size. On the other hand, if the static S/N ratio were to be 100, then  $p$  would have a value of 10, and the error rate for even a 1 pixel-sized defect would be only 15%.



Note: For various values of the tool operating parameter  $p = \{C.(S/N)\}$  and assuming an *OTF* with the form shown in Figure 3.

**Figure 4 Computed Error Rates as a Function of Defect Size (in Pixels)**

#### 4 APPLICATION OF THEORY TO DEFECT REVIEW TOOLS

The SEMATECH workshop in February suggested that a desirable performance metric for a next generation E-beam defect review tool would be a 50% error rate for 10 nm defects, 20% for a 40 nm defect, and 10% for a 130 nm defect. To see how close to reality this sort of specification might be, this paper will make some further assumptions about the likely properties of an current E-beam tool. The incident beam current  $I_B$  is related to the spot size  $d$  of the tool by the relation:

$$I_B = 1.88\beta \frac{d^{8/3}}{C_s^{2/3}} \quad \text{Eq. [5]}$$

where  $\beta$  is the brightness of the electron gun (in amps/cm<sup>2</sup>/steradian) and  $C_s$  is the spherical aberration coefficient of the probe forming lens (in cm.). For this example,  $\beta$  will be taken to be 10<sup>6</sup> amps/cm<sup>2</sup>/str. and  $C_s$  will be set to 5 mm. These figures are plausible estimates of the type of performance that might be achievable with a Schottky field emitter gun, at 2 keV, in an optimized tool. From these numbers, and using Eq. [5], the probe sized for incident beam currents of 0.1, 1.0, and 10 nA corresponding to the values used in Figure 2, then can be calculated to be 7, 16, and 37 nm, respectively. It can be noted that these probe currents and

beam sizes are consistent with the quoted specification of the KLA SEM-SPEC for operation at 2 keV (KLA 1996).

The error-rate analysis developed above now can be applied to the KLA SEM-SPEC operating at 2 keV. Following the KLA specification, the probe and pixel size are set to 0.05  $\mu\text{m}$ , the field of view is  $512 \times 512$  pixels in size, the beam current is then 25 nA, and the pixel time is 10 ns. The signal-to-noise ratio S/N for silicon is then about 25 from Eq. [3] and so for a defect with a contrast of 10% the parameter  $\mathbf{p} = \{(S/N).C\}$  is 2.5. From Figure 4, it can then be seen that a 400 nm (i.e., an 8-pixel) defect would be detected with an error rate of below 10%, while a 150 nm (3-pixel) defect would be detectable with a 35% error rate. Under these conditions, the wafer could be scanned (ignoring any overhead for signal processing or sample movement) at a rate of  $2.5 \times 10^{-3} \text{ cm}^2/\text{sec}$  or about  $9 \text{ cm}^2/\text{hour}$ . These estimates of performance are in good agreement with the typical error rates and throughput speeds actually reported for this tool, confirming that the model is realistic.

The analysis now can be applied to a more advanced system. For defects at future technology nodes, a smaller probe size and a correspondingly reduced beam current must be used. Using the instrumental parameters derived earlier, it can be seen that a beam of size 16 nm can be obtained with a beam current of 1 nA. The pixel size of the scanned field will be assumed also equal to 16 nm, and the pixel acquisition time will be increased to 1  $\mu\text{s}$  to compensate for the reduction in current. The S/N ratio then will be about 50, and so for the defect with a contrast of 0.1 the parameter  $\mathbf{p}$  will be 5. From the data of Figure 4, it can be seen that the error rate for a 130 nm (i.e., an 8-pixel) defect would be only 0.02%, while a 40 nm (i.e., a 3-pixel) defect would have an error rate of 25%. A 10 nm defect is below one pixel in size, and so must be taken to be undetectable (i.e., error rate of 50%).

Superficially, this looks promising as these defect sizes and error rates match or exceed the suggested specifications from the February SEMATECH workshop. However, with a  $512 \times 512$  scanned area of 16 nm pixel size, and a 1  $\mu\text{s}$  pixel time, the wafer is being scanned at the rate of  $2 \times 10^{-6} \text{ cm}^2/\text{sec}$ . or about  $9 \times 10^{-3} \text{ cm}^2/\text{hour}$ , compared to the target specification value of 10–200  $\text{cm}^2/\text{hour}$ . Thus, although using currently available technology, there is no problem in detecting the smallest defects, the gap in performance between the desired rate and the achievable rate at which wafers can be scanned, under the assumptions used above, is three to four orders of magnitude.

It should be noted that simple geometric considerations account for almost all of this shortfall in performance. If the pixel size is reduced by a factor of M times to accommodate smaller defect sizes, then  $M^2$  more pixels must be scanned to cover the same area, hence the process will take  $M^2$  as long as previously. In addition, if the probe size is maintained equal to the pixel size, then a reduction in the pixel size of M times also will require a reduction in the probe size by a factor of M. Hence, from Eq. [5], the incident beam current will fall by a factor of at least  $M^2$ . In order to maintain the same error rate, it therefore is necessary to increase the dwell time per pixel by a factor of  $M^2$ . As a result, a reduction in desired defect size by M times will lead to an increase of  $M^4$  in the time required to scan a given area of the device.

#### 4.1 What Can be Done to Improve the Performance

In view of the large gap between the desired performance and the above estimate of currently achievable performance, it is necessary to examine which portions of the tool could be replaced to try to close this gap.

### 4.1.1 Brighter Electron Sources

From Eq. [2], it is clear that the S/N ratio at all spatial frequencies can be improved by enhancing the electron source brightness. Since current tools already use Schottky or cold field emitters, which offer a very high brightness, only a technology capable of offering at least an order of magnitude in brightness would be worth considering. The only technology likely to achieve that level of increase in performance is the atomic size nano-tip field emitter, which can provide an improvement of between 10X and 100X (Schmid and Fink 1997 [10]). Such a factor would be a useful improvement, but each order of magnitude increase in source brightness would only increase reading speed of the tool by a factor of three times, so at best only about one order of magnitude can be gained in this manner. Much more practical work also remains to be done to make nanotips a viable commercial source and to extract their best performance under routine operating conditions, so this approach is not yet a commercial reality.

Since the brightness of an emitter increases linearly with beam energy, it might seem that increasing the accelerating voltage from 2 to 20 keV would be of value. Indeed, it is reported for the KLA SEM-SPEC that operation at 20 keV rather than 2 keV results in an increase of 10X in the probe current. But, as noted above, the secondary electron yield of most materials falls by about a factor of 5X to 10X over the same energy range (Joy 1999 [3]), and thus there is little net gain in reading speed for a given defect size and error rate. Consequently, increasing the beam energy is not a productive strategy for enhancing throughput, especially as increased beam energies often are implicated in beam damage. Defects in the size range 100–130 nm can be captured using a dose of about 5000 electrons, which corresponds to a dose of about 0.1 electrons/Å<sup>2</sup> for a 16 nm pixel size. Except at the lowest energies, this is too low to cause permanent radiation damage, but may result in surface contamination or charging.

### 4.1.2 Electron–Optical Improvements

The model system analyzed above assumes a lens with a spherical aberration coefficient  $C_s$  of 5 mm, and a correspondingly low chromatic aberration value. However, considerably better performance than this is now possible. In particular, by making the probe forming lens a “cathode lens” in which an initially high energy beam (20 keV) is slowed down to 2 keV or less, and by employing advanced design techniques and high excitation values,  $C_s$  can be reduced to 0.3 mm or less while still maintaining a physical working distance of 1 to 2 mm (Hordon et al., 1995 [2]). With this reduction in  $C_s$ , the numerical aperture (NA) of the lens can be increased by a factor of four to five times while still keeping the same probe size, and as a result the beam current will increase by a factor of about 20X. A still greater improvement could be achieved with a corrector device that could lower  $C_s$  and  $C_c$  to below 0.1 mm (e.g., Rose 1996 [9]). By fully exploiting such improvements in imaging optics, an increase in the reading speed of about five to ten times would be possible, but the downside of this improvement is that there would be a corresponding reduction in the usable depth of field (DOF) of the tool. Thus, for a 16 nm pixel size and a high performance lens operating at 2 keV with a  $C_s$  of 0.3 mm, the aperture angle would be about 30 milliradians and the DOF would be about 500 nm (0.5 μm). Depending on the flatness of the wafer and the aspect ratios of the structures being examined, this figure might be uncomfortably small. A reduced DOF also imposes requirements for greater accuracy on the auto-focus system of the tool which could in turn exact a penalty on performance.

### 4.1.3 Better Detectors

As shown in Eq. [3] the detector quantum efficiency (*DQE*) directly affects the signal-to-noise ratio and hence the error rate for a given set of operating conditions. The *DQE* of a typical “through-the-lens” secondary electron detector is about 0.6 to 0.8, while the *DQE* of an asymmetrically mounted Everhart-Thornley detector is in the range 0.2 to 0.5 ( Nakasuji and Shimizu, 1996 [8], Joy et al., 1996 [4]). There is, therefore, little potential for gaining any major improvement in observation speed by enhancing the efficiency detectors of current microscopes. However, modifications to detectors to make them more specific to a particular type of electron, or contrast event, might lead to an increase in the contrast of a defect, and hence to a reduction in the error rate.

### 4.1.4 Multiple Columns/Detectors

The earlier SEMATECH workshop report suggests that “an army of micro-SEMS is now feasible and could be THE solution for speed.” There is, of course, no question that the use of many electron-beam columns, independently working in parallel on the same sample, would increase the scanning speed for defects. It is also true that this approach appears to offer a safe and relatively well guaranteed route to substantially higher performance since, other than the possibility of crosstalk between the systems, most of the required technology is already in existence (Koops et al., 1995 [5], Liu et al., 1996 [7]). In the short term, however, there are significant practical problems to overcome, specifically as follows:

1. Micro-columns typically run at currents of the order of 10–100 pA (rather than 10 nA), so scan rates will have to be slower to maintain acceptable error rates.
2. The optics of a micro-column are far less optimized than those of the systems discussed above, resulting in lower currents into a given probe diameter.
3. The efficiency of the detector associated with each column will have to be controlled to prevent unwanted signal leakage from adjacent columns, so possibly reducing the S/N ratio for any given condition.
4. The emitters in a micro-column are typically not user-replaceable, and so if one fails that particular column is of no further use.

These considerations suggest that although a large array (the number *N* in the range 1000 to 10,000) of columns certainly would have a significant speed advantage compared to a single column, the magnitude of this gain probably would be substantially less than a factor of *N* times that of a fully optimized single column. To achieve the speed gain of about 10,000X that is required to match the SEMATECH target specification, it seems probable that perhaps 20,000 or more columns would be required to provide enough performance and sufficient redundancy to handle failures. While 20,000 is not an impossible number if it could be monolithically fabricated by standard device technologies, there are certainly practical problems that will require attention, such as providing scanning, video amplification, and data analysis for this number of columns.

## 5 CONCLUSIONS

This discussion above shows the following:

1. The SEMATECH specification set for the detection of small (<100 nm) at acceptable error rates can be met readily using technology that is already available.
2. However, the scanning rate that is possible for such sub-100 nm defects is about three to four orders of magnitude slower than required.

An analysis of the options available shows that this gap can be partially closed as follows:

1. By using higher brightness electron sources such as nanotip field emitters, offering a factor of up to 10X in speed
2. By employing advanced lenses and electron-optical schemes, such as retarding field cathode lenses, possibly yielding another factor of 10X in scan speeds

However, these options, employed separately or together, still can only accelerate the reading rate to reach a few percent of the desired value, and side effects such as a reduced DOF and increased charging even then might make the procedure unacceptable. The only “conventional” solution that could, in principle, guarantee the desired reading speed is the use of massively parallel arrays of micro-columns. While this is on the edge of feasibility, much work will have to be undertaken to make this a technology suitable for fab-line operation, and a significant level of redundancy will have to be provided in any such system to ensure long-term reliability at the required performance level.

### 5.1 Is There An Alternative?

The final question therefore, remains: Is there some radically different approach that could avoid the problems that limit the performance of the conventional scanned beam system?

One potential solution is the use of reflection electron holography performed in a point projection microscope (Kreuzer et al., 1992 [6]). A coherent beam of low energy (<500 eV) electrons produces an illumination footprint a few micrometers in diameter on the surface of the wafer. Electrons scattered from the surface interfere with unscattered electrons to produce a Fresnel hologram of the surface at the detector plane. The magnification of the image is simply the ratio of the distance from the sample to the detector divided by the distance from the source to the sample. No lenses are required, so the spatial resolution of the image reconstructed from this hologram is limited only by the number of pixels in the detector, and ultimately by the wavelength of the electrons.

At imaging magnifications of 20,000X, and for a detector with only  $100 \times 100$  pixels, a resolution of better than 10 nm is attainable. The simplicity of this arrangement is in contrast to the complexity of a conventional, SEM-like instruments and indicates that the cost of ownership (COO) of such a tool could be highly competitive. The hologram is preferable to a simple image because it contains all of the information required to reconstruct the three-dimensional configuration of the surface. Additionally, the hologram is sensitive to such effects as potentials on the surface and so will respond to “voltage contrast” in defects. The sensitivity of the hologram to surface information depends on the signal-to-noise ratio that can be achieved, and so for high performance operation an ultra-bright electron source such as a “nanotip” will be mandatory.

Because the entire area is illuminated simultaneously, the burden of achieving a high reading speed is shifted from the scanning system to the data acquisition and analysis system. Since a hologram is a linear vector representation of the amplitude and phase of the wavefront leaving the sample surface, rather than being the scalar intensity of the signal as is the case for a conventional image, differences between a test area and a reference golden area can be performed directly by subtracting the holograms. Any residual between two holograms therefore represents the existence of defects; the position, size, and shape of which can be obtained by reconstructing the hologram. The detection of a defect, therefore, does not require pattern recognition technology. When specific information on a defect is required, the difference hologram can be reconstructed by Fourier transformations. Since pattern recognition is a relatively slow process; while Fourier transforms can be performed at very high speed by specialized hardware, it seems likely that the holographic approach will have a significant speed advantage.

Replacing imaging by holography, and scanning beam microscopy by the point projection microscope, represents a radical shift in technology and consequently considerable work needs to be done to prove the viability of the technique, particularly when it is applied to complex, high aspect-ratio structures. If these tests are successful, however, point projection holography would be a defect review technique that could deal with any technology node yet envisaged.

## 6 REFERENCES

- [1] Brundle C. R., Uritsky Y., Kinney P., Huber W., and Green A. (1998) in *Characterization and Metrology for ULSI Technology*, editor D. G. Seiler et al., 677.
- [2] Hordon L. S., Boyer B. B. and Pease R.F. W. (1995), *J. Vac. Sci. Technology*, B13, 826.
- [3] Joy D. C. (1999) – For a complete database on Electron-Solid interactions see <http://web.utk.edu/~srcutk>.
- [4] Joy D. C., Joy C. S., and Bunn R. (1996), *Scanning* 18, 533.
- [5] Koops H. W. P., Munro E., Rouse J., Kretz J., Rudolph M., Weber M., and Dahm G. (1995), *Nucl. Instrum. Meth. in Physics*, A363, 1.
- [6] Kreuzer H. J., Nakamura K., Wierzbich A., Fink H.-W., and Schmid H. (1992), *Ultramicroscopy*, 45, 381.
- [7] Liu W., Ambe T., and Pease R. F. W. (1996), *J. Vac. Sci. Technology*, B14, 3738.
- [8] Nakasuji M. and Shimizu H. (1996), *J. Electr. Microsc.*, 45, 359.
- [9] Rose H. (1996), *Proc. Ann. Meeting MSA*, ed. B. Bailey (Springer Verlag:New York), 233.
- [10] Schmid H. and Fink H.-W. (1997), *Appl. Phys. Lett.*, 70, 2679.



**SEMATECH Technology Transfer  
2706 Montopolis Drive  
Austin, TX 78741**

**<http://www.sematech.org>  
e-mail: [info@sematech.org](mailto:info@sematech.org)**